Supporting Information for "Stratospheric age of air variations between 1600-2100"

S. Muthers,[1,2], A. Kuchar[3,4], A. Stenke[3], J. Schmitt[1,2], J. G. Anet[5], C. C. Raible[1,2], T. F. Stocker[1,2]

Corresponding author: S. Muthers, Physics Institute, Climate and Environmental Physics, Sidlerstrasse 5, CH-3012 Bern, Switzerland. (muthers@climate.unibe.ch)

[1]Climate and Environmental Physics, University of Bern, Bern, Switzerland.

[2]Oeschger Centre for Climate Change Research, University of Bern, Bern, Switzerland.

[3]Institute for Atmospheric and Climate Science, ETH, Zurich, Switzerland

[4]Department of Atmospheric Physics, Faculty of Mathematics and Physics, Charles University in Prague

[5]Suisse Federal Laboratories for Material Science and Technology (Empa) Duebendorf, Switzerland

Contents of this file

Method: Superposed epoch analysis

The strongest eruptions of the simulation period 1620 – 2100 are chosen to estimate the influence of volcanic aerosols on Age of Air (AoA) in a superposed epoch analysis. During this period, all eruptions with an annual mean aerosol optical depth (AOD) of 0.1 or larger are selected from the volcanic forcing reconstruction [*Arfeuille et al.*, 2014]. The resulting 10 volcanic eruptions are summarized in Table S2.

For each volcanic eruption the AoA anomalies after the eruptions are calculated relative to the average AoA value of the five years before the eruption took place. These five years represent volcanically unperturbed AoA values. For the eruption of Tambora (1815), however, the period 1810 to 1814 is substantially affected by the unknown 1809 eruption. For this case, the years 1805 to 1808 are chosen as the reference period. Similarly, for the eruption of Cosiguina (1835) a small influence of preceding eruption of Babuyan Claro (1831) may exist. However, with an AOD of 0.09 this eruption is small in size and no long-lasting effects on AoA were found.

For each year after the eruption, the AoA anomaly is then averaged over all simulations and eruptions to estimate the mean response. Furthermore, the standard deviation across all simulations and eruptions is calculated as a measure of the variability.

Methods: Removal of the volcanic signal from AoA

Episodic events, like volcanic eruptions, are usually difficult to consider in a multiple linear regression analysis. Therefore, the influence of volcanic eruptions is removed from the AoA time series and the remaining residual is used to detect the influence of CO_2, ozone depleting substances, and the solar forcing.

To remove the volcanic influence from the AoA time series, a statistical relationship between AOD and AoA is calculated using the 10 strongest eruptions during the period 1620-2100 (Table S2). Using these 40 eruptions (4 simulations $\times$ 10 eruptions) we calculate a linear regression between the AOD value of the first eruption year and the AoA anomaly (calculated as described in superposed epoch analysis) for year 1 to year 5. The linear model is then used to predict the AoA response to each volcanic eruption during the first five years and this value is removed from the original time series. The results of this approach are shown in Fig. S5, with the black line resembling the original global mean AoA and the red line showing the residuum after removal of the volcanic signal.

For the regression pattern analysis, where the zonal mean 3-D AoA field is used, the volcanic signal is removed in a similar way. First the statistical model between AoA and AOD is constructed for every latitude and pressure level, then the predicted response is removed from the original data, when a statistically significant effect of AOD on AoA is detected at this location.

References

Andrews, D. G., J. R. Hinton, and C. B. Leovy (1987), *Middle atmosphere dynamics*, 489 pp., Academic Press, Orlando, USA.

Arfeuille, F., D. Weisenstein, H. Mack, E. Rozanov, T. Peter, and S. Brönnimann (2014), Volcanic forcing for climate modeling: A new microphysics-based data set covering years 1600–present, *Climate of the Past*, *10*(1), 359–375, doi:10.5194/cp-10-359-2014.

Butchart, N., A. A. Scaife, M. Bourqui, J. Grandpré, S. H. E. Hare, J. Kettleborough, U. Langematz, E. Manzini, F. Sassi, K. Shibata, D. T. Shindell, and M. Sigmond (2006), Simulations of anthropogenic change in the strength of the Brewer–Dobson circulation, *Climate Dynamics*, *27*, 727–741, doi:10.1007/s00382-006-0162-4.

Table S1. Overview of the experiments used in this study.

Name	Period	# Simulations	Forcings
STRONG	1600-2100	2	all forcings, large TSI amplitude, RCP 4.5
MEDIUM	1600-2100	2	all forcings, medium TSI amplitude, RCP 4.5
CONST	2000-2100	2	all forcing, constant 11-yr solar cycle, RCP 4.5
DM-REF	1780-1840	3	constant 1780
DM-UV	1780-1840	3	UV variations only, other forcings: constant 1780
DM-nonUV	1780-1840	3	non-UV variations only, other forcings: constant 1780

Table S2. Overview of the volcanic eruptions considered in this study, including the year of the eruption, the maximum annual mean aerosol optical depth (AOD), and the name and latitude of the volcano. Note, for the eruptions of the year 1693, 1883, and 1991 the maximum annual mean AOD is found in second year of the eruption.

Year (AD)	AOD	Description
1641	0.11	Parker (Philippines 6°N)
1693	0.11	Serua (Indonesia 6°S)
1719	0.13	unknown
1809	0.23	unknown
1815	0.27	Tambora (Indonesia, 8°N)
1835	0.20	Cosiguina (Nicaragua, 13°N)
1883	0.12	Krakatau (Indonesia, 6°S)
1963	0.11	Agung (Indonesia, 8°S)
1991	0.12	Mt. Pinatubo (Philippines, 15°N)
2060	0.11	artificial Agung-like eruption

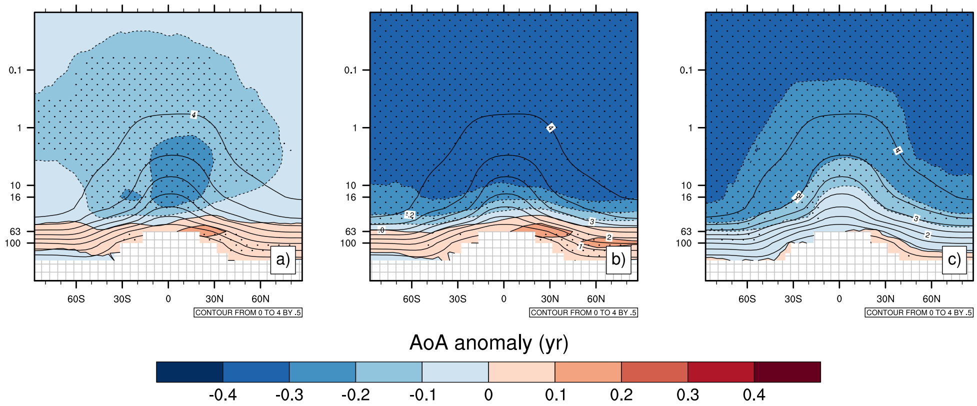

Figure S1. Annual mean AoA anomalies for the 10 strongest volcanic eruptions of the period 1620 to 2100. **(a)** year of the eruptions, **(b)** first and **(c)** second year after the start of the eruption. Contours denote the climatological annual mean AoA during the period 1620 to 2100. Significantly different anomalies are indicated by stippling (Students t-test, $p \leq 0.05$).

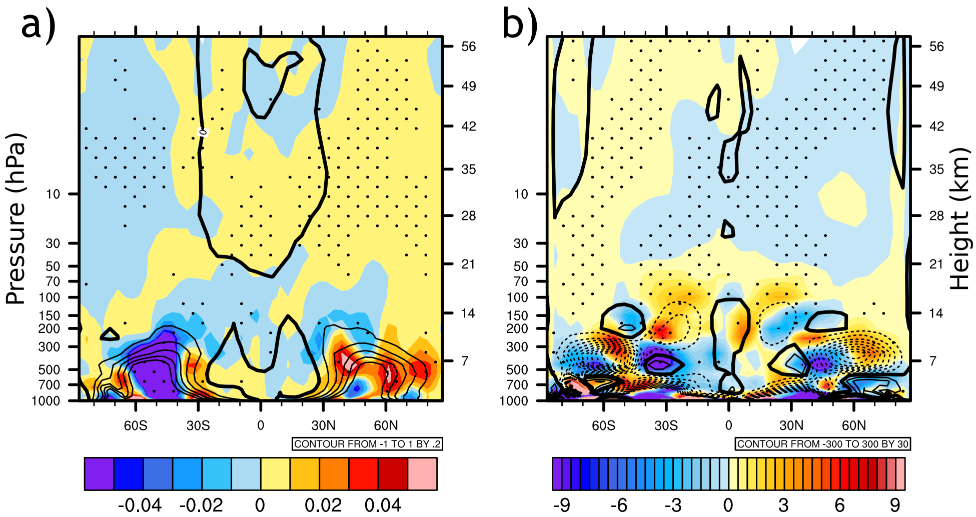

Figure S2. Eliassen-Palm (EP) flux [*Andrews et al.*, 1987] anomalies during the first eruption year in the volcanic eruption composite: **(a)** Vertical component of the EP-flux ($10^4\,\mathrm{kg\,s^{-2}}$), **(b)** EP-flux divergence ($\mathrm{kg\,m^{-1}\,s^{-2}}$). Contours denote the values of the reference period, composite calculation as described above. Significant different anomalies are indicated by stippling (Students t-test, $p \leq 0.05$).

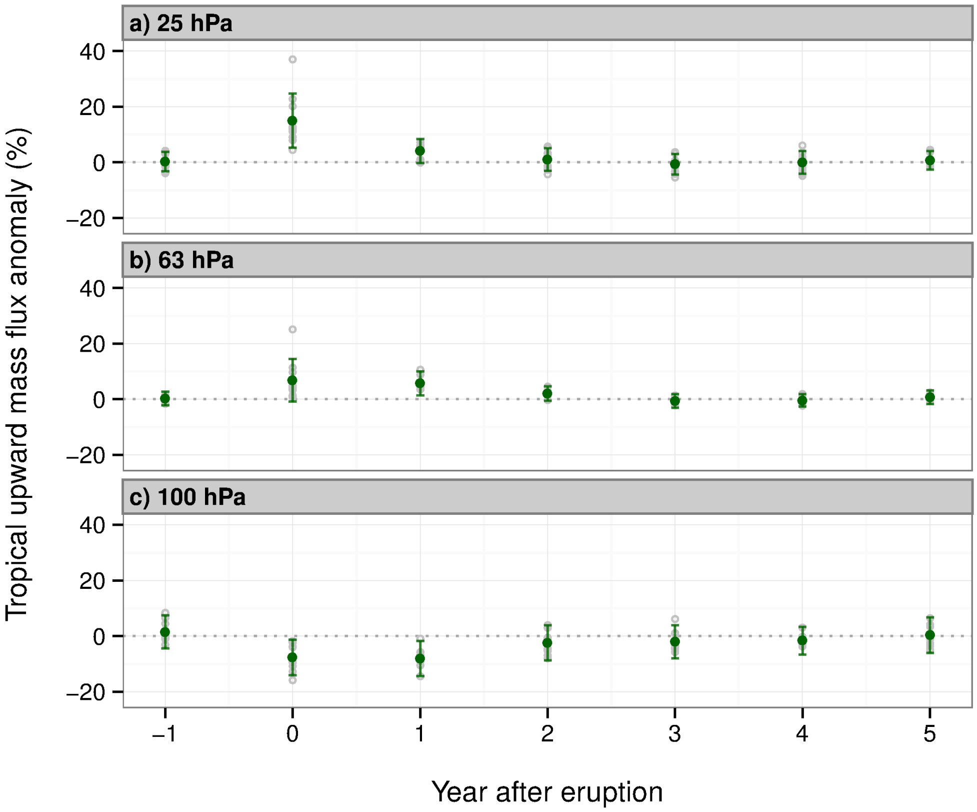

Figure S3. Volcanic composite for the annual mean tropical upward mass flux anomalies after strong volcanic eruptions for different altitudes (**a**: 25 hPa, **b**: 63 hPa, **c**: 100 hPa). The average over all eruptions and experiments in shown by the green dots with the bars indicating the ensemble standard deviation. Thin gray points represent the individual simulations and eruptions. The tropical upward mass flux is calculated by integrating the monthly mean massflux over all latitudes between 60°S and 60°N when the vertical residual velocity at this latitude is positive (upward) [compare *Butchart et al.*, 2006]. For comparison, the preindustrial (< 1900) tropical upward massflux corresponds to $35{\cdot}10^8$kg/s, 74 $\cdot10^8$kg/s, and $152{\cdot}10^8$kg/s, for the levels 25 hPa, 63 hPa, and 100 hPa, respectively.

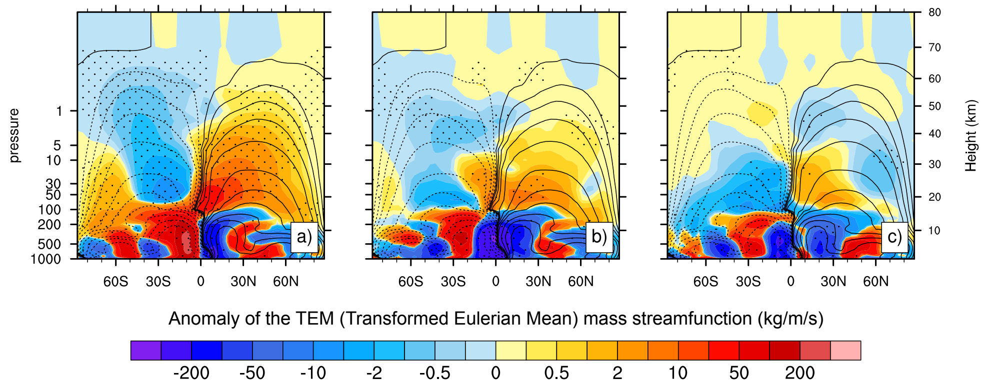

Figure S4. Volcanic composite of the transformed Eulerian mean (TEM) mass streamfunction for the (a) eruption year, (b) the first, and (c) the second year after the beginning of the eruption. Contour lines denote the mean values of the reference period and are log-spaced from from -5000 to 5000 kg/m/s. Coloured contours denote the log-spaced anomalies, reaching from -500 to 500 kg/m/s. Stippling indicates significant differences to the reference ensemble (Student's t-test, $p \leq 0.05$).

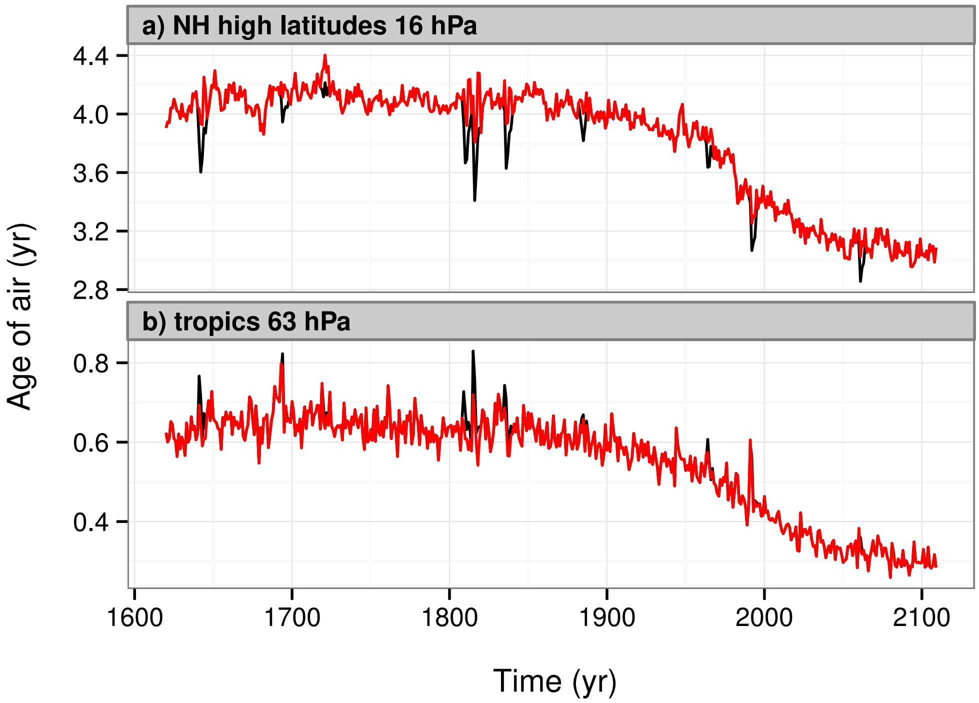

Figure S5. Ensemble mean (strong solar only) AoA from 1620 to 2100 **(a)** in the middle stratosphere of the NH high latitudes and **(b)** in the tropical lower stratosphere. In black the original values are shown. The red line denotes the remaining AoA variations, when the influence of volcanic eruptions is removed.

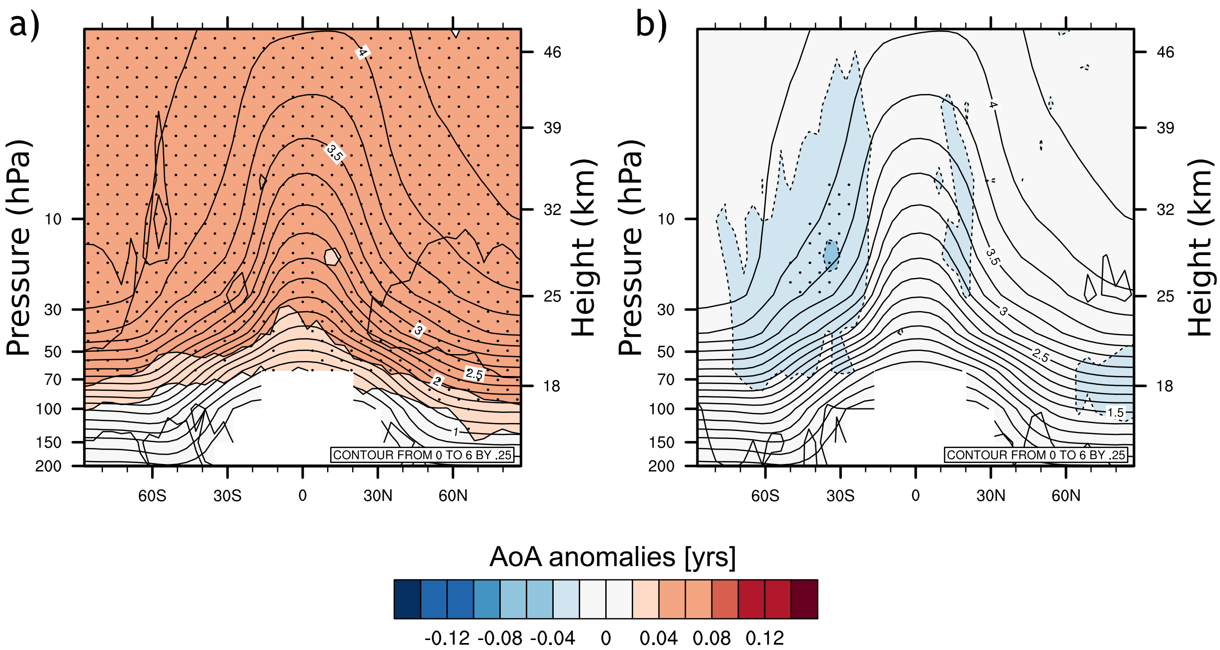

Figure S6. AoA anomalies in the Dalton Minimum sensitivity experiments driven by **(a)** non-UV and **(b)** UV variations only. The anomalies are averaged over the period 1805-1815, the differences are calculated against an ensemble of reference simulations with constant 1780 conditions. Stippling indicates significant differences to the reference ensemble (Student's t-test, $p \leq 0.1$). Contours denote the mean AoA in the reference ensemble.

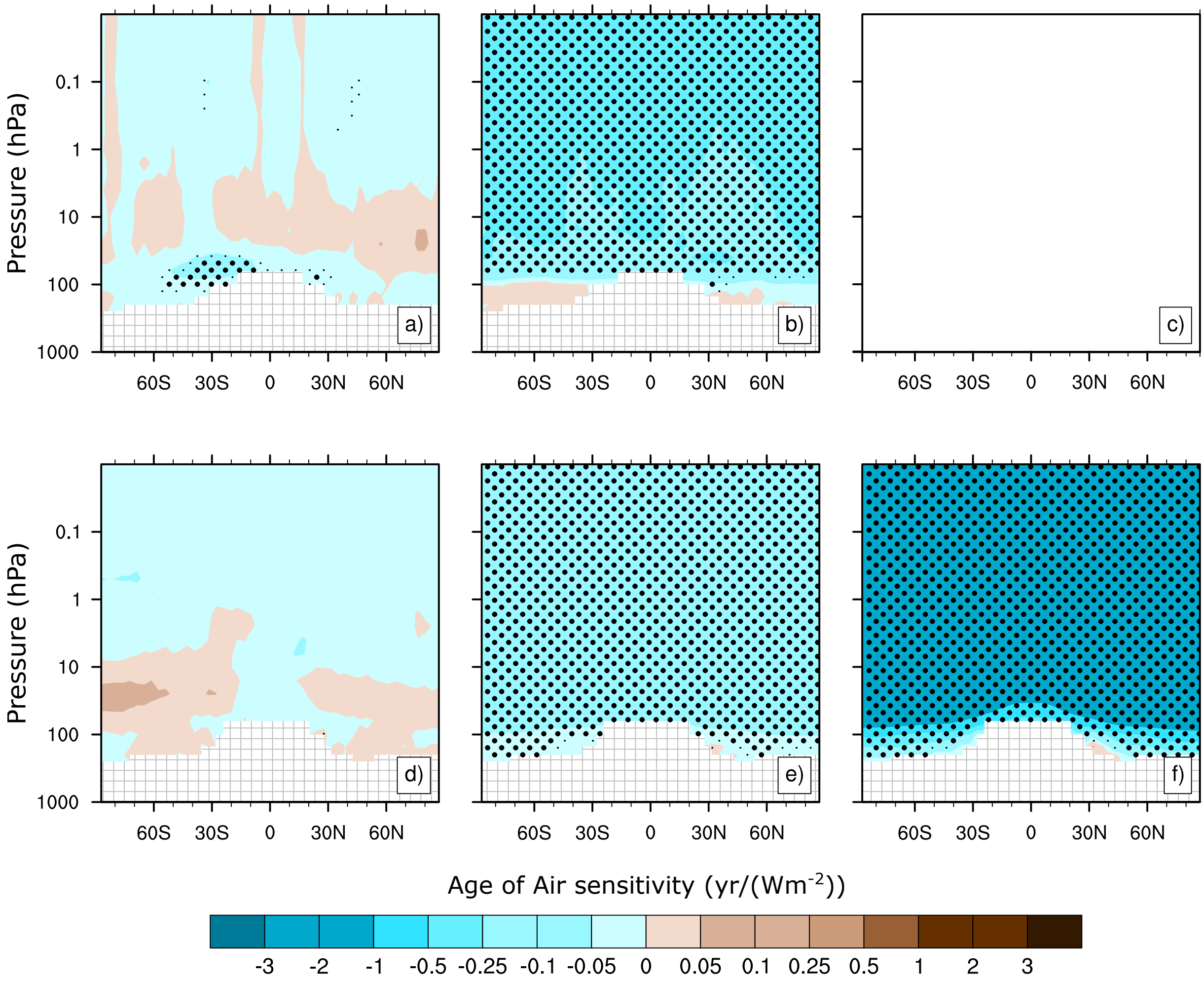

Figure S7. Similar to Fig. 3 but separated for preindustrial (1620–1899) and modern (1900–2100) periods. **a-c:** Multiple linear regression coefficients over the period 1620–1899 for TSI (**a**), CO_2 (**b**), and ODS (**c**). **d-e:** Multiple linear regression coefficients over the period 1900–2100 for TSI (**d**), CO_2 (**e**), and ODS (**f**). Stippling indicates significant regression coefficients (thick stippling: $p \leq 0.05$, smaller stippling $p \leq 0.1$).